Resource

Chemistry & Biology

Optogenetic Control of Molecular Motors and Organelle Distributions in Cells

Graphical Abstract

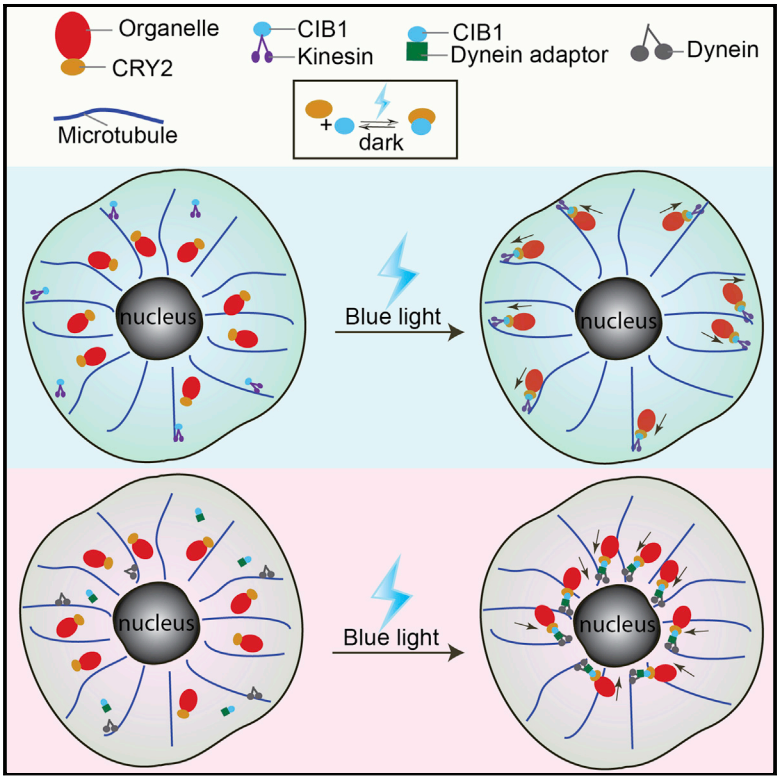

Authors

Liting Duan, Daphne Che, ..., Shunling Guo, Bianxiao Cui

Correspondence

bcui@stanford.edu

In Brief

Based on the heterodimerization of cryptochrome 2 and CIB1, Duan et al. develop an optogenetic tool to control organelle distribution in cells by light-inducible recruitment of molecular motors to organelle outer membrane.

Highlights

- We developed an optogenetic tool to control organelle distributions in cells
- Motor proteins can be recruited to organelle membrane by dimerization of CRY2-CIB1
- Organelles can be driven toward cell nucleus or toward cell periphery by light
- Light-induced organelle transport can be spatially controlled at subcellular region

Duan et al., 2015, Chemistry & Biology 22, 671–682
May 21, 2015
http://dx.doi.org/10.1016/j.chembiol.2015.04.014

CellPress

Chemistry & Biology
Resource

Optogenetic Control of Molecular Motors and Organelle Distributions in Cells

Liting Duan,[1,3] Daphne Che,[1,3] Kai Zhang,[1,2] Qunxiang Ong,[1] Shunling Guo,[1] and Bianxiao Cui[1,*]
[1]Department of Chemistry, Stanford University, Stanford, CA 94305, USA
[2]Department of Biochemistry, University of Illinois at Urbana-Champaign, Urbana, IL 61801, USA
[3]Co-first author
*Correspondence: bcui@stanford.edu
http://dx.doi.org/10.1016/j.chembiol.2015.04.014

SUMMARY

Intracellular transport and distribution of organelles play important roles in diverse cellular functions, including cell polarization, intracellular signaling, cell survival, and apoptosis. Here, we report an optogenetic strategy to control the transport and distribution of organelles by light. This is achieved by optically recruiting molecular motors onto organelles through the heterodimerization of *Arabidopsis thaliana* cryptochrome 2 (CRY2) and its interacting partner CIB1. CRY2 and CIB1 dimerize within subseconds upon exposure to blue light, which requires no exogenous ligands and low intensity of light. We demonstrate that mitochondria, peroxisomes, and lysosomes can be driven toward the cell periphery upon light-induced recruitment of kinesin, or toward the cell nucleus upon recruitment of dynein. Light-induced motor recruitment and organelle movements are repeatable, reversible, and can be achieved at subcellular regions. This light-controlled organelle redistribution provides a new strategy for studying the causal roles of organelle transport and distribution in cellular functions in living cells.

INTRODUCTION

In mammalian cells, important proteins and organelles are actively transported to their appropriate locations by a two-way microtubule-based traffic system. In this system, the molecular motors dyneins and kinesins convert chemical energy into mechanical work to deliver cargoes. Dyneins walk toward the minus end of microtubules and thus carry cargoes to the cell nucleus. In the opposite direction, kinesins walk toward the plus end of microtubules and take cargoes to the cell periphery. Accumulating evidence indicates that distinct spatial distributions of organelles exist under defined conditions and play important roles in various cellular functions in cells. For example, it is observed that nutrients induce peripheral positioning of lysosomes while starvation causes perinuclear clustering of lysosomes (Korolchuk et al., 2011). Localization of the mitochondria to the vicinity of plasma membrane is proposed to be crucial for sustained Ca^{2+} influx across plasma membrane and T-cell activation (Quintana et al., 2006; Schwindling et al., 2010). On the other hand, the perinuclear clustering of mitochondria, observed during hypoxia, is proposed to be indispensable for high levels of nuclear reactive oxygen species under hypoxia and regulation of hypoxia-induced gene expression (Al-Mehdi et al., 2012). At the subcellular level, non-symmetric transport and distribution of organelles are crucial for the development and functioning of highly polarized cells (Mellman and Nelson, 2008). For example, in cultured hippocampal neurons, the preferential delivery of post-Golgi vesicles to an immature neurite biases the morphological polarization of the neurite into an axon (Bradke and Dotti, 1997). However, a direct link between organelle distributions and cellular functions is missing, due to the lack of effective and controllable means to manipulate organelle transport in living cells.

A desirable method to control the organelle distribution in cells should have the following characteristics. First, it should be able to be conducted in living cells so that the functional consequences of organelle redistribution can be investigated in vivo. Second, it should be reversible so that the regulation can be stopped at a desired time point. Finally, it should permit temporal and spatial control to study intracellular activities in certain temporal patterns and/or in distinct subcellular regions. Recently, a rapamycin-induced FKBP-FRB heterodimerization system has been developed that enables inducible recruitment of molecular motors to specific organelles and drives organelle redistribution inside the cell (Kapitein et al., 2010a, 2010b; van Spronsen et al., 2013). This technique provides the unique capability of controlling organelle distribution in living cells. However, it requires a rapamycin cofactor, which needs to penetrate the cell membrane and cannot be applied with subcellular precision. In addition, the rapamycin-induced binding is not reversible.

The rapidly emerging area of optogenetic actuators provides new opportunities to control motor activities and organelle redistribution. Several pairs of light-induced dimerization proteins have been developed, including the light-oxygen-voltage (LOV) domain (Harper et al., 2003; Renicke et al., 2013; Strickland et al., 2010, 2012; Wu et al., 2009), phytochrome B (Levskaya et al., 2009; Shimizu-Sato et al., 2002; Toettcher et al., 2013), and cryptochrome 2 (CRY2) (Bugaj et al., 2013; Kennedy et al., 2010). Among these, the CRY2 and the LOV systems do not need exogenous cofactors for dimerization. In a very recent study, the light-induced heterodimerization between the LOV2 domain from *Avena sativa* phototropin 1 and an engineered PDZ domain was utilized to optically control organelle redistribution (van Bergeijk et al., 2015). Using a similar strategy, here we

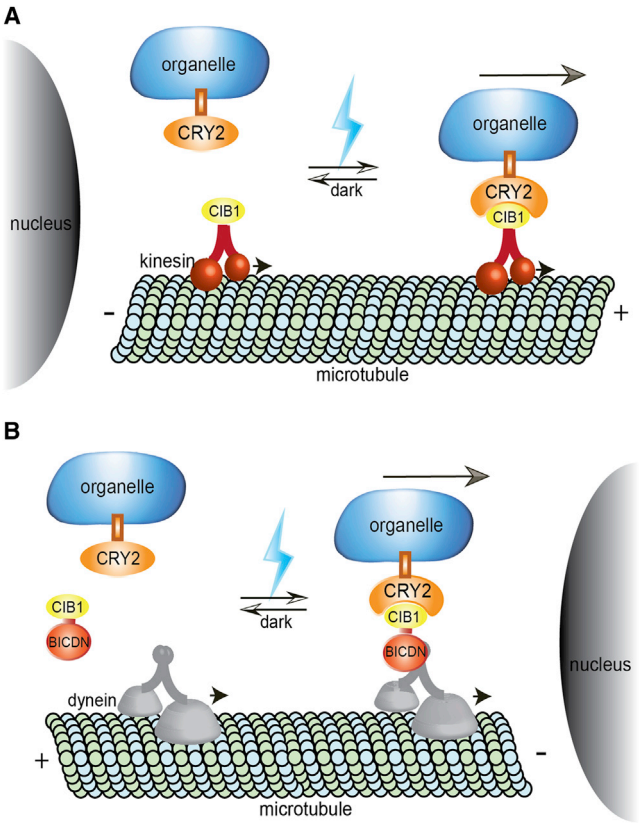

Figure 1. Schematic of Light-Controlled Motor Recruitment and Organelle Transport in Cells

(A) CRY2 is anchored to organelles via a specific organelle-targeting transmembrane domain. CIB1 is linked to truncated kinesin KIF5A. Upon blue-light exposure, CIB1-CRY2 binding recruits kinesin motors to organelles, which drives organelles toward the plus end of the microtubule.

(B) CIB1 domain is linked to BICDN, a dynein/dynactin adaptor protein. When illuminated with blue light, CIB1 binds with CRY2 and thus recruits dynein to organelles. Consequently, organelles are propelled toward the minus end of the microtubule.

exploit the light-controlled binding of CRY2 to its interacting partner CIB1 to achieve optogenetic control of organelle redistribution in living cells. Previously, light-inducible CRY2-CIB1 binding has been used to control endogenous transcription (Konermann et al., 2013), phosphoinositide metabolism (Idevall-Hagren et al., 2012), and activation of signaling pathways such as Raf/MEK/ERK (Zhang et al., 2014) and PI3K signaling pathway (Kakumoto and Nakata, 2013). The light-induced heterodimerization of CRY2-CIB1 requires a low level of light and thus introduces minimal light toxicity in long-term studies (Zhang et al., 2014). By tethering CRY2 to specific organelles and CIB1 to molecular motors, we demonstrate light-induced transport of organelles to the perinuclear region by recruiting dyneins, and light-induced transport of organelles to the cell plasma membrane by recruiting kinesins. The strategy is generally applicable to many types of organelles including mitochondria, peroxisomes, and lysosomes. The manipulation of organelle distribution is reversible, and spatial control of organelle distribution can be achieved in subcellular regions.

RESULTS

Design Scheme for Optogenetic Control of Molecular Motors and Organelle Distribution

We have designed a generic method that uses light to control motor recruitment to organelle membrane, and thus controls organelle distributions in living cells. Intracellular transport of organelles is mainly propelled by microtubule-based motor proteins including kinesins and dyneins. It was previously reported that by utilizing the FKBP-rapalog-FRB heterodimerization system, recruitment of motors can drive specific cargo movement and organelle redistribution (Kapitein et al., 2010b). Inspired by this study, we hypothesized that reversible and spatial control of inducible organelle movement could be achieved if we were able to use light to recruit motors to specific organelles. To this end, we chose the CRY2-CIB1 heterodimerization module that can bind within subseconds in the presence of blue light and dissociate within a few minutes of turning off the blue light. In this study, we used the photolyase homology region of CRY2 (amino acids 1–498) and N-terminal region of CIB1 (amino acids 1–170) (Kennedy et al., 2010). In our design (Figure 1), CRY2 was localized to different organelles via cargo-specific membrane linkers while to control motors, CIB1 was fused to either KIF5A, a truncated kinesin protein, or BICDN, the N terminus of the dynein/dynactin interacting protein BICD. Truncated kinesin KIF5A without the tail domains is known to be unable to bind to cargoes (Cai et al., 2007). When truncated KIF5A are recruited to organelles upon CRY2/CIB1 dimerization under blue light, the organelles should move toward the plus ends of the microtubules, which are mostly localized at the cell periphery. On the other hand, the recruitment of BICDN to organelles will recruit dynein motors and induce transport of organelles toward the minus ends of microtubules, which usually reside around the cell nucleus.

Light Induces Redistribution of Cellular Mitochondria by Recruiting Molecular Motors

We first demonstrated that mitochondria could be moved toward the perinuclear region by light-induced recruitment of BICDN. Throughout this study, intermittent 200-ms exposure of blue light at 9.7 W/cm^2 per 10-s interval was used to stimulate the dimerization of CRY2-CIB1 unless otherwise noted. CRY2 was targeted to mitochondria by CRY2-mCherry-MiroTM, where MiroTM is the transmembrane domain of Miro1, a component of the motor/adaptor complex that anchors to the mitochondria outer membrane (Fransson et al., 2006). The specific mitochondria localization of CRY2-mCherry-MiroTM was confirmed by the co-localization between CRY2-mCherry-MiroTM and Mito-YFP, a known mitochondria targeting sequence from cytochrome *c* oxidase (Rizzuto et al., 1989) (Figure S1). As shown in Figure 2A, in the COS-7 cell co-transfected with CRY2-mCherry-MiroTM and GFP-BICDN-CIB1, some mitochondria were positioned close to the nucleus while others spread throughout the cell. The distribution of GFP-BICDN-CIB1 in the same cell was cytosolic and diffusive (Figure 2B). After intermittent stimulation with blue light for 1 hr, mitochondria became highly clustered around cell nucleus (Figure 2A), driven by light-recruited dynein motors (Movie S1 shows the transport dynamics). The cytosolic distribution of GFP-BICDN-CIB1 in this cell did not change upon blue-light illumination

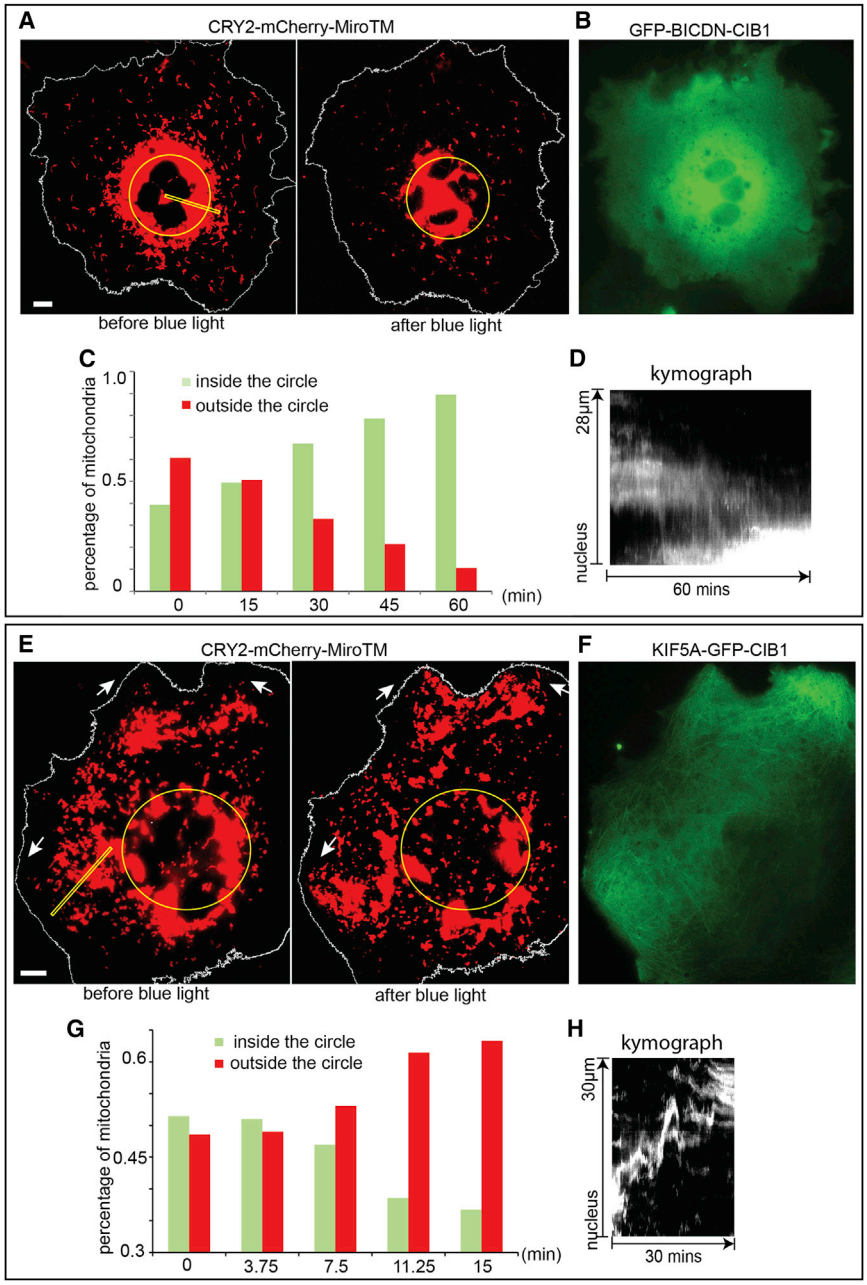

Figure 2. Light-Induced Redistribution of Mitochondria in COS-7 Cells by Recruiting Molecular Motors

(A–D) The COS-7 cell was transfected with CRY2-mCherry-MiroTM and GFP-BICDN-CIB1. (A) Mitochondria were visualized in the red channel by CRY2-mCherry-MiroTM. Before blue-light illumination, some mitochondria were positioned close to the nucleus while others were spread throughout the cell. After blue-light illumination, most mitochondria moved toward the cell nucleus as indicated by the yellow circle (n = 20). (B) The green channel showed GFP-BICDN-CIB1 diffusing in the cytosol. (C) The percentage of mitochondria inside the yellow circle in (A) increased from 39% to 89% after intermittent light exposure for 60 min. (D) The kymograph extracted from the area indicated by yellow rectangle in (A) showed the clear trend of mitochondria moving toward the nucleus.

(E–H) The COS-7 cell was transfected with CRY2-mCherry-MiroTM and KIF5A-GFP-CIB1. (E) After blue-light illumination, many mitochondria moved away from the perinuclear region (yellow circle) and some clustered at the cell edge, as indicated by the arrows (n = 73). (F) KIF5A-GFP-CIB1 in the same cell distributed along the microtubules. (G) The percentage of mitochondria at the perinuclear region (inside the yellow circle) decreased from 52% to 36% after intermittent light exposure for 30 min. (H) The kymograph extracted from the area indicated by yellow rectangle in (E) showed that over time, mitochondria were actively moved toward the cell periphery.

Scale bars, 10 μm. See also Figure S2; Movies S1 and S2.

(Figure S2A), likely due to the much higher expression of cytosolic GFP-BICDN-CIB1 than mitochondria-localized CRY2-mCherry-MiroTM. Indeed, the co-localization between GFP-BICDN-CIB1 and CRY2-mCherry-MiroTM was observed in cells with very low expression levels of GFP-BICDN-CIB1 (Figures S2B–S2E). To quantify the global mitochondria movements, the percentage of mitochondria inside the yellow perinuclear circle was calculated at different time points using a MATLAB program (Experimental Procedures; Figure S3). The perinuclear circle was set to enclose the whole nucleus. The diameter was adjusted to include approximately 50% fluorescence intensity of the whole cell at the beginning of the experiment, which gives the best contrast if organelles move in or out of the circle. In the cell shown in Figure 2A, before blue-light illumination, only 39% of mitochondria were localized inside the circle. Over the 60-min intermittent illumination of blue light, the percentage of mitochondria inside the circle gradually increased to 89% (Figure 2C). The kymograph extracted from the time-lapse movie (along the yellow rectangle in Figure 2A) demonstrated that mitochondria were actively transported to the proximity of the cell nucleus (Figure 2D).

Likewise, we showed that mitochondria could be moved outward to the cell periphery by light-induced recruitment of KIF5A (Figures 2E–2H; Movie S2). The COS-7 cell was co-transfected with CRY2-mCherry-MiroTM and KIF5A-GFP-CIB1. Unlike GFP-BICDN-CIB1, which was diffusive, KIF5A-GFP-CIB1 retained the microtubule binding affinity of kinesin, and its distribution showed microtubule tracks (Figure 2F). Upon blue-light illumination, mitochondria spread out toward the cell periphery and some clustered at the cell edge as indicated by the white arrows in Figure 2E. KIF5A-GFP-CIB1 distribution in this cell did not change noticeably after exposure to blue light (Figure S2F). The percentage of mitochondria inside the yellow circle gradually decreased from 52% to 36% after blue-light illumination for

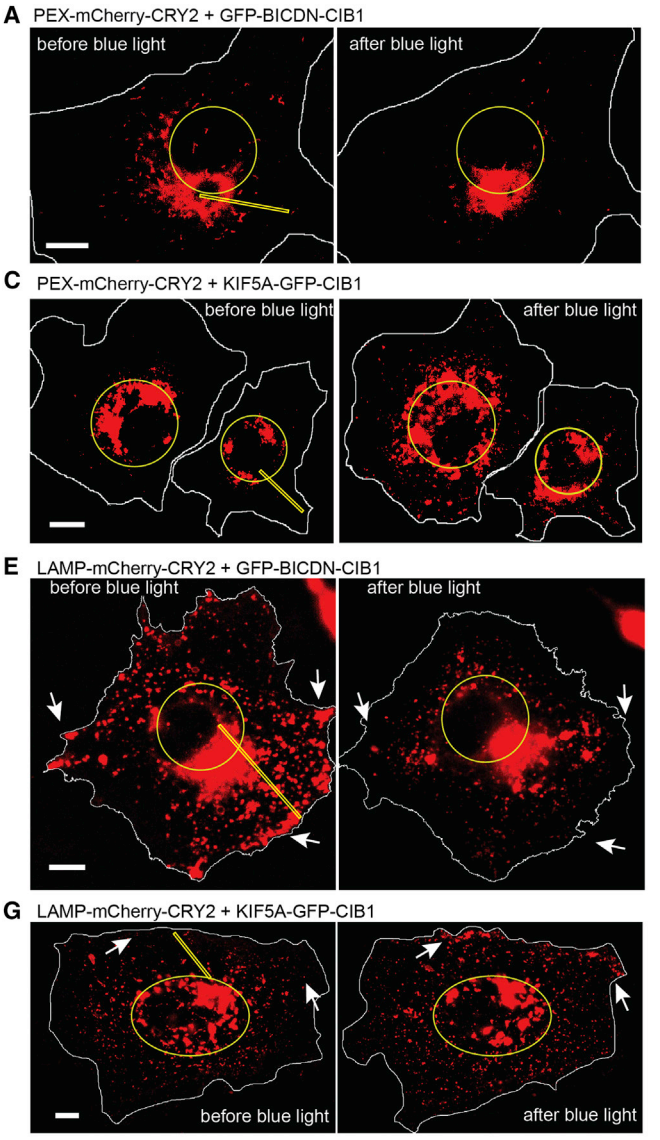

Figure 3. The Distributions of Peroxisomes and Lysosomes in Cells Can Be Modulated by Light-Induced Recruitment of Motors

(A) In the cell co-transfected with GFP-BICDN-CIB1 and PEX-mCherry-CRY2, blue-light illumination caused peroxisomes to become highly clustered around the cell nucleus indicated by the circle.

(B) The kymograph generated along the yellow rectangular region in (A) shows the trajectories of peroxisomes moving toward the nucleus.

(C) In the cell transfected with KIF5A-GFP-CIB1 and PEX-mCherry-CRY2, blue-light illumination caused peroxisomes to move away from the cell nucleus. The circles mark the cell nuclei.

(D) The kymograph generated along the yellow rectangular region in (C) shows peroxisomes moving away from the nucleus.

(E) In the cell transfected with GFP-BICDN-CIB1 and LAMP-mCherry-CRY2, blue-light illumination induced lysosomes clustering around the nucleus marked by the yellow circle. The amount of lysosomes near the cell edge was drastically reduced as indicated by the white arrows.

(F) The kymograph generated along the yellow rectangular region in (E) shows lysosomes moving toward the nucleus.

(G) In the cell transfected with KIF5A-GFP-CIB1 and LAMP-mCherry-CRY2, lysosomes moved toward the cell periphery upon exposure to blue light. The cell nucleus is indicated by the ellipse. The amount of lysosomes near the cell edge was drastically increased as indicated by the white arrows.

(H) The kymograph generated along the yellow rectangular region in (G) shows lysosomes moving toward the cell periphery.

Scale bars, 10 μm. See also Figure S5.

15 min (Figure 2G). The kymograph along the yellow rectangular region indicated that mitochondria were actively transported toward the cell periphery during light illumination (Figure 2H).

As negative controls, without blue-light stimulation, COS-7 cells co-transfected with either CRY2-mCherry-MiroTM and GFP-BICDN-CIB1 or KIF5A-GFP-CIB1 and CRY2-mCherry-MiroTM did not show significant change in mitochondria spatial distribution after 1 hr (Figures S4A and S4B). Furthermore, in co-transfected cells that lacked CIB1 (i.e. CRY2-mCherry-MiroTM and GFP-BICDN, CRY2-mCherry-MiroTM and KIF5A-GFP) or in cells single-transfected with CRY2-mCherry-MiroTM, mitochondria distribution did not change after stimulation with blue light for 1 hr (Figures S4C–S4E).

Multiple Types of Organelles Can Be Relocated by Light-Induced Recruitment of Motors

In addition to the ability to induce redistribution of mitochondria, our method can also initiate directional transport of other organelles by tethering CRY2 to their outer membranes. In this regard, we attached CRY2 to the membrane of peroxisomes by linking to the N terminus of PEX (amino acids 1–42), which is the peroxisome membrane-targeting domain of a peroxisomal membrane protein (Kammerer et al., 1998). In the cell transfected with PEX-mCherry-CRY2 and GFP-BICDN-CIB1 (as shown in Figure 3A), some peroxisomes were located close to the nuclear region and some were distributed throughout the cell. After intermittent exposure to blue light for 37 min, almost all peroxisomes were relocated very close to nucleus. The kymograph in Figure 3B showed the clear trend of peroxisomes moving toward the nucleus. In the opposite microtubule direction we demonstrated that, in the cell transfected with PEX-mCherry-CRY2 and KIF5A-GFP-CIB1 shown in Figure 3C, blue-light stimulation drove the peroxisomes toward the cell periphery, similar to the behavior of mitochondria described in the previous section. After 25 min of blue-light stimulation, the distribution of peroxisomes was much more spread out in the cell compared with before blue-light stimulation. The kymograph shown in Figure 3D (generated from the yellow rectangle in Figure 3C) clearly showed the trend of peroxisome cargoes moving outward. The distribution of

GFP-BICDN-CIB1 and KIF5A-GFP-CIB1 did not change after light-induced peroxisome redistribution (Figures S5A and S5B).

We also demonstrated the optogenetic control of cargo distribution for lysosomes. To activate the light-induced movement of lysosomes, mCherry-CRY2 was fused to the N terminus of LAMP, an integral membrane protein specific to lysosomes (Chen et al., 1988). When blue light was turned on, the recruitment of BICDN to lysosomes resulted in translocation of lysosomes to the perinuclear region in COS-7 cells co-transfected with GFP-BICDN-CIB1 and LAMP-mCherry-CRY2 (Figure 3E). In particular, the amount of lysosomes near the cell edge was drastically reduced as indicated by the white arrows, corroborated by the kymograph in Figure 3F. On the other hand, the light-induced recruitment of KIF5A-GFP-CIB1 to lysosomes resulted in lysosome translocation to the cell periphery (Figures 3G and 3H). The distribution of GFP-BICDN-CIB1 and KIF5A-GFP-CIB1 did not change obviously after light-induced lysosome redistribution (Figures S5C and S5D).

We noticed that the instantaneous moving speeds of translocation were similar for mitochondria, lysosomes, and peroxisomes. However, the redistribution of peroxisomes, on average, occurred much faster than mitochondria when induced by blue-light exposure. We also noticed that most light-induced mitochondria movements were in zigzag and stop-and-go patterns (see Movies S1 and S2), while peroxisomes moved more smoothly over large distances and in straight lines (see Movies S3 and S4). One possibility is that peroxisomes are smaller in size than mitochondria and thus maneuver more easily through a dense cellular environment. It is also possible that some mitochondria are tethered to cellular structures, e.g. cytoskeleton (Boldogh and Pon, 2006), and are not able to be moved even when molecular motors are recruited to them. The successful demonstration of light-induced organelle movement and redistribution of mitochondria, peroxisomes, and lysosomes shows that our method is generally applicable to induce polarized transport and differential distribution patterns of different organelles in cells.

Light-Recruited Molecular Motors Move along Microtubules

Although light-induced recruitment of molecular motors drives organelle redistribution, it is of interest to know whether the artificially recruited motors retain their native properties. Therefore, we investigated whether motors recruited via a CRY2-CIB1 dimerization system move along microtubules, and also measured the speeds of cargo movement propelled by these artificially recruited motors. For this purpose, we chose peroxisomes as cargoes because they are smaller and fewer in number than mitochondria or lysosomes, which makes it easier to track their individual cargo movements. First, we showed that light-induced recruitment of kinesins resulted in peroxisome transporting along microtubules. Cells were triple-transfected with PEX-mCherry-CRY2, KIF5A-CIB1, and TAU-YFP, among which TAU-YFP was used to label microtubules (Samsonov et al., 2004). In this section, KIF5A-CIB1 was not labeled with any fluorescence tag. Figure 4A shows that a peroxisome moved along a microtubule after blue-light stimulation and headed toward the plus end of the microtubule that pointed to the cell edge. The overlap could be seen more clearly in the maximum-intensity Z projection of the time-lapse movie.

Next, we examined the movement speed of individual peroxisomes by blue-light recruitment of KIF5A (Figure 4B). In cells transfected with PEX-mCherry-CRY2, KIF5A-CIB1, and TAU-YFP, we recorded time-lapse movies at 1 frame/s for peroxisome movement over a period of 400 s. Z projection of the movie yielded peroxisome trajectories that demonstrated an outward radial distribution overlapping with some microtubules. Interestingly, we often observed many peroxisomes moving on the same microtubules (Movie S3). Two kymographs (Figure 4C) were generated along the two microtubules shown as yellow rectangles in Figure 4B. There were, respectively, 8 and 16 peroxisomes transporting along these two microtubules in 250 s (Figure 4C). However, peroxisomes seemed to move on selected subsets of microtubules, and only a small fraction of cellular microtubules were used. Throughout the 400-s movie acquisition, only around 50 out of hundreds of microtubules had peroxisomes moving on them. Most peroxisomes moved along these trajectories continuously and at a relatively constant speed. We measured the moving speeds of 177 peroxisomes, and the distribution of transport velocity showed a mean value at 0.55 μm/s with a spread between 0 and 2.0 μm/s (Figure 4D).

Next, we also confirmed that light-induced dynein recruitment drove cargoes moving along microtubules. In Figure 4E, the cell triple-transfected with BICDN-CIB1, TAU-YFP, and PEX-mCherry-CRY2 showed a region where many microtubule ends merged as the arrow indicates, likely a microtubule-organizing center. Blue-light illumination triggered the retrograde transport of peroxisomes, which resulted in the accumulation of peroxisomes at the microtubule nucleation site (Movie S4). The trajectories of peroxisomes in the Z-projection image clearly overlap with the microtubule patterns surrounding the microtubule nucleation site. Kymographs were generated from the two trajectories indicated as (III) and (IV), and showed that peroxisomes moved along the microtubules toward the cell center (Figure 4F). Transport speeds of 119 peroxisomes in four cells were measured and presented as the histogram of speeds in Figure 4G, showing a mean value at 0.57 μm/s and a spread from 0 to 2.0 μm/s (Figure 4G). The average speed for peroxisome transport driven by light-induced molecular motor recruitment in this study is in line with speed measurements reported in a previous in vivo peroxisome transport study (Kural et al., 2005).

Light-Induced Organelle Redistribution Is Reversible

Reversibility is a highly desirable property for the regulation of motor activity and organelle transport. Here, we showed that the binding of molecular motors and light-induced movement of mitochondria were reversible upon turning off the blue light. First, we demonstrated that binding between CRY2 and CIB1 on mitochondria was reversible using cells co-transfected with CIB1-GFP-MiroTM and CRY2-mCherry. To demonstrate the CRY2-CIB1 binding reversibility we use organelle-localized CIB1 and cytosolic CRY2 instead of organelle-localized CRY2 and cytosolic CIB1, because CRY2 usually has a much lower expression level than CIB1. Binding of CRY2-mCherry to organelle-localized CIB1 will visually deplete cytosolic CRY2 and thus, the co-localization can be clearly observed. In this experiment, during blue-light illumination the cell was stimulated with a 200-ms exposure of blue light at 9.7 W/cm^2 per 1-s interval. As shown in Figure 5A, the initially diffusive and cytosolic

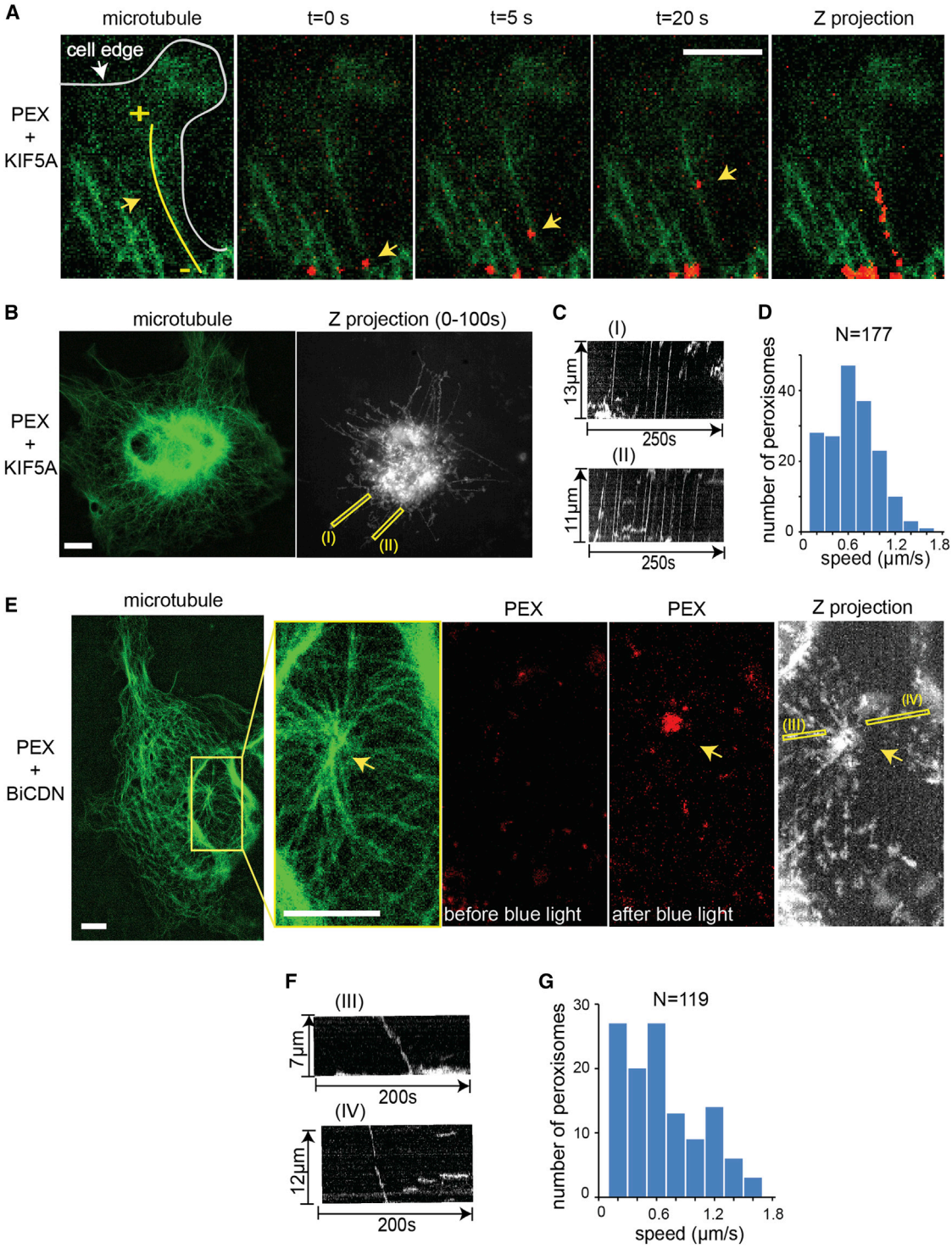

Figure 4. Characterization of Organelle Transport by Light-Induced Recruitment of Molecular Motors

(A) The peroxisome indicated by the yellow arrow moved along the microtubule and toward the cell periphery by light-induced recruitment of kinesins. The cell was triple-transfected with KIF5A-CIB1, TAU-YFP, and PEX-mCherry-CRY2. Microtubules were labeled by TAU-YFP. Z projection of peroxisomes was obtained by projecting the maximum intensity of PEX-mCherry-CRY2 during 20-frame acquisition at 1 frame/s and was merged with the GFP image, which overlaps with the underlying microtubule.

(B) Z projection of light-induced peroxisome trajectories spreads radially from the nucleus to the cell periphery, resembling the distribution of the microtubule network. The cell was triple-transfected with KIF5A-CIB1, TAU-YFP, and PEX-mCherry-CRY2. Z projection of peroxisomes was obtained by recording the maximum intensity of PEX-mCherry-CRY2 during 100-frame acquisition at 1 frame/s.

(legend continued on next page)

CRY2-mCherry were quickly recruited to mitochondria after blue-light illumination. The CIB1-CRY2 binding is reversible after the blue light is turned off, and the process is highly repeatable. Figure 5B shows four consecutive cycles of the CIB1-CRY2 association/dissociation in the yellow rectangular area indicated in the cell (see Movie S5). The CYR2-CIB1 binding was usually completed within 10 s while the dissociation took around 10 min. Such repeated process did not change the binding/unbinding dynamics.

We also demonstrated that the light-induced mitochondria redistribution was reversible (Figure 5C). In the cell transfected with KIF5A-GFP-CIB1 and CRY2-mCherry-MiroTM, mitochondria were observed to move away from nucleus with light-induced recruitment of kinesins. In this cell, the percentage of mitochondria inside the yellow circle was 61% initially and dropped to 40% after blue-light illumination. However, during the following 3-hr incubation in darkness, more and more mitochondria moved back toward the cell nucleus and the percentage increased from 40% to 63%. After 10 min of incubation in the dark, CRY2 and CIB1 would dissociate and, thus, kinesins would be no longer bound to mitochondria. Afterward, other motors such as dyneins or myosins may bind to mitochondria and drive them back toward the cell nucleus. We noted that not all light-induced organelle redistribution was reversible within the 3-hr time frame we were measuring, suggesting complex intracellular processes.

We found that the expression level of KIF5A affected the overall rate of light-induced organelle redistribution, whereas the expression level of BICDN did not. We compared light-induced mitochondria redistribution in cells with different motor expression levels but with similar MiroTM (cargo) expression levels. Before and after blue-light illumination for 15 min, the average distance of mitochondria movement was calculated using a custom-written MATLAB program (see Experimental Procedures for details). Figure 5D shows the movement of 20 cells at different KIF5A levels. It is clear that the higher was the KIF5A expression level, the further the mitochondria moved toward the cell periphery. Therefore, more KIF5A motors recruited to mitochondria will drive mitochondria further in the same time frame. On the other hand, the expression level of BICDN did not appear to affect the moving distance of mitochondria. It is likely that in cells transfected with GFP-BICDN-CIB1, the translocation of mitochondria is limited by the total amount of endogenous dyneins.

Organelle Redistribution Can Be Spatially Controlled at Subcellular Regions

The optogenetic control affords high spatial resolution, and we demonstrated that light-induced mitochondria movement can be spatially controlled at subcellular regions. First, we showed that CRY2/CIB1 heterodimerization can be controlled spatially in the cell co-transfected with CRY2-mCherry and CIB1-GFP-MiroTM (Figure 6A). When blue light was restricted to the circled area, CRY2-mCherry was observed to co-localize with mitochondria only in the circled subcellular area, while CRY2-mCherry remained diffusive and cytosolic in the rest of the cell. After the subcellular recruitment demonstration the entire cell was subsequently illuminated with blue light and CRY2-mCherry was observed to co-localize with mitochondria throughout the cell, indicating that the previous subcellular recruitment of CIB1-GFP-MiroTM was indeed due to the restricted light illumination.

Next, we demonstrated that the distribution of organelles can be spatially controlled by confining the illumination area to subcellular regions. As shown in Figure 6B, the cell was co-transfected with CRY2-mCherry-Miro1TM and KIF5A-GFP-CIB1. Before any blue-light illumination, there were few mitochondria in the proximity of cell membrane. Blue light was confined to the marked area and illuminated for 1 min. Mitochondria in the illuminated area were observed to move out toward the cell membrane, while in other areas the mitochondria remained mostly stationary. To confirm that mitochondria in other areas could also be translocated by light, we removed the spatial restriction. After the blue light activated the whole cell for 15 min, the outward movement of mitochondria was seen throughout the cell.

DISCUSSION

We have developed a method to optically control directional transport and redistribution of organelles in living cells by utilizing light-induced CRY2-CIB1 interaction. Light-induced recruitment of kinesins initiates the transport of organelles to plus ends of microtubules (toward the cell edge) while light-induced recruitment of dynein adaptors propels organelles toward minus ends (toward the cell nucleus). Light-induced redistributions of multiple types of organelles have been demonstrated, including mitochondria, peroxisomes, and lysosomes. The use of light as a control switch provides unique advantages. First, light-induced CRY2-CIB1 binding is reversible, which is highly desirable for reversible motor recruitment and organelle redistribution. The reversibility also ensures complete termination of light-inducible motor recruitment in the absence of blue light, thus providing an end point of regulation. Second, light affords highly localized spatial control. We have demonstrated that the organelles in the light-illuminated subcellular area became motile while organelles in non-illuminated areas remained unchanged (Figure 6). The spatial control of motor activities and organelle movement would be particularly important in investigating the cargo transport in polarized cells, which are structurally and functionally asymmetric.

(C) Kymographs of the indicated yellow rectangles (I) and (II) in (B) show that many peroxisomes moved toward the cell periphery on the same microtubules and at a relatively constant speed.
(D) Histogram of peroxisome speed for 177 peroxisomes in four cells shows an average speed of 0.55 μm/s.
(E) Trajectories of light-induced peroxisome retrograde movement resemble the distribution of microtubules around the center (indicated by the arrow) where many microtubules merged. The cell was triple-transfected with BICDN-CIB1, TAU-YFP, and PEX-mCherry-CRY2.
(F) Kymographs of the indicated rectangles (III) and (IV) show that peroxisomes moved along microtubules toward the cell nucleus.
(G) Histogram of peroxisome speed obtained by calculating the speeds for 119 peroxisomes in four cells shows an average speed of 0.57 μm/s.
Scale bars: 5 μm (A), 10 μm (B, E). See also Movies S3 and S4.

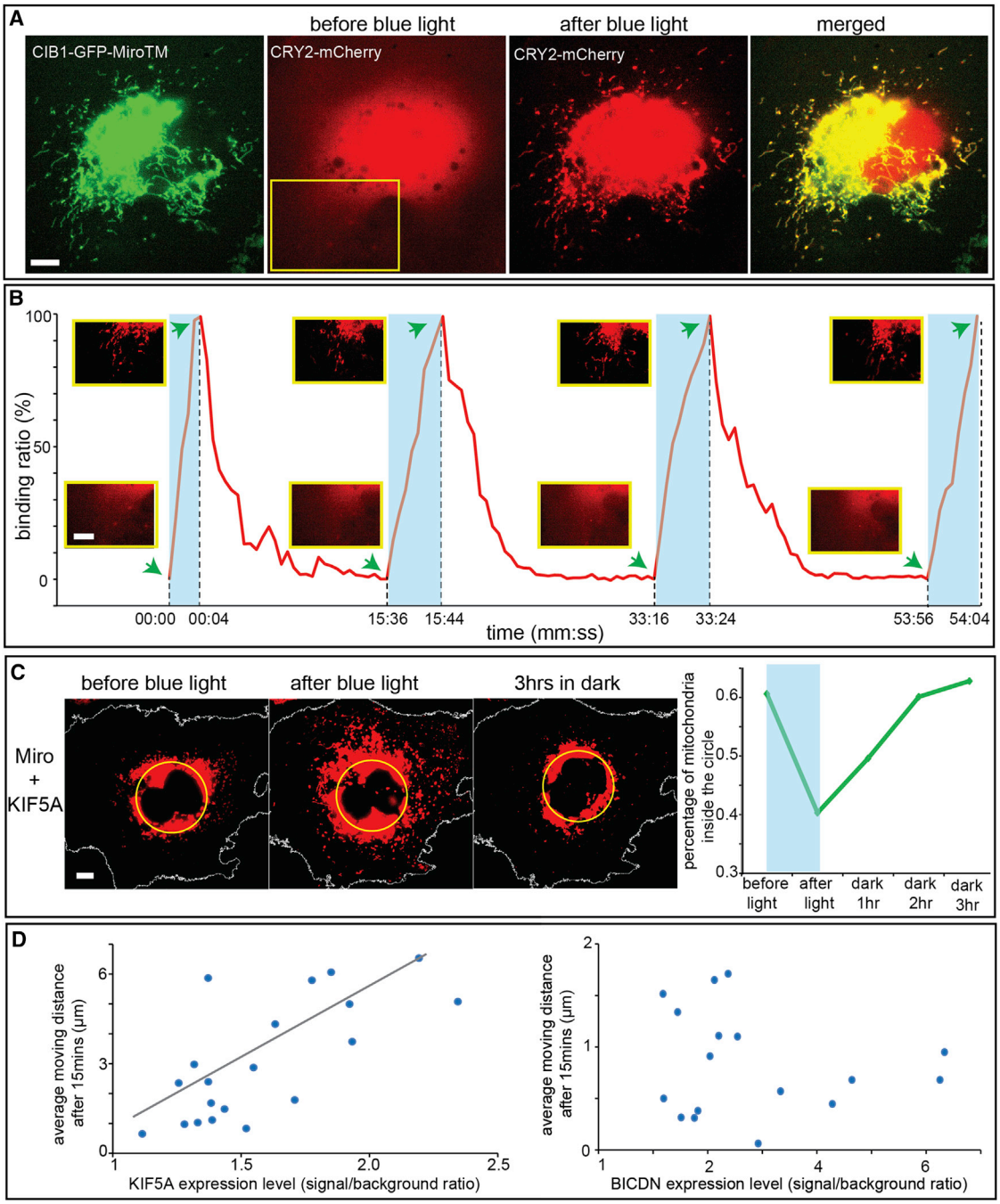

Figure 5. Light-Induced Organelle Redistribution Is Reversible and Is Dependent on Motor Expression Level

(A) CRY2 and CIB1 binding on mitochondria membrane is reversible and repeatable. The cell was transfected with CIB1-GFP-Miro1TM and CYR2-mCherry. Before blue light, CIB1-GFP-Miro1TM was targeted to mitochondria while CYR2PHR-mCherry was cytosolic. Upon blue-light exposure, CRY2-mCherry bound to CIB1-GFP-Miro1TM and localized to mitochondria.

(B) The same transfected cell shown in (A) was repeatedly subjected to four cycles of blue light and dark periods. For each cycle, CRY2-mCherry was recruited to mitochondria within seconds of blue-light illumination, and returned to its cytosolic distribution after incubating in the dark for 10–15 min. Within each period of blue-light illumination, the cell was stimulated with 200-ms exposure of blue light at 9.7 W/cm^2 per 1-s interval. Each image of CRY2-mCherry was taken at the time point indicated by the green arrow.

(C) In the cell transfected with CRY2-mCherry-MiroTM and KIF5A-GFP-CIB1, mitochondria were driven toward the cell periphery by intermittent blue-light exposure (one 200-ms pulse per 10 s) for 30 min. The cell was then incubated without blue-light stimulation, and mitochondria were observed to gradually move back toward the cell nucleus. Quantification of the percentage of the mitochondria inside the yellow circle shows the percentage decreased from 61% to 40% after blue-light stimulation and increased back to 63% after 3 hr incubation in the dark.

(legend continued on next page)

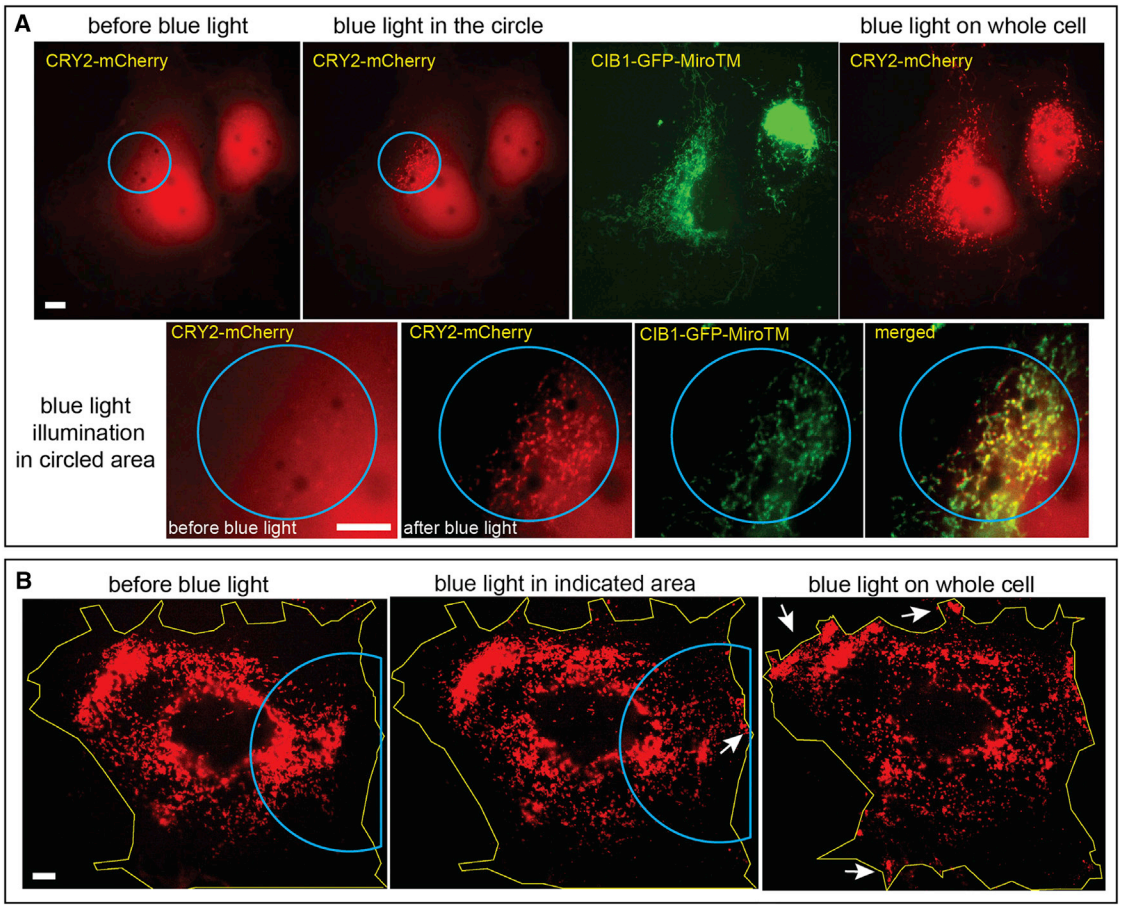

Figure 6. Subcellular Spatial Control of Light-Induced Mitochondria Movement

(A) The COS-7 cell was transfected with CRY2-mCherry and CIB1-GFP-MiroTM. Blue-light illumination was restricted within a subcellular region of the cell (indicated by the blue circle). Upon blue-light activation, CRY2-mCherry was recruited to mitochondria only in the targeted region, whereas it remained cytosolic in the rest of the cell. The local recruitment can be more clearly seen in the zoomed-in images shown in the lower panel. Later, the whole cell was illuminated with blue light and CRY2-mCherry became co-localized with mitochondria in the whole cell (rightmost image).

(B) In the cell co-expressing CRY2-mCherry-MiroTM and KIF5A-GFP-CIB1, only the marked region was illuminated with intermittent blue light for 1 min at 5-s intervals. Only in this region, mitochondria moved outward to the cell periphery, as indicated by the white arrow, while in the remaining part of the cell mitochondria distribution remained mostly unchanged (middle image). Later, the whole cell was illuminated with intermittent blue light for 15 min, and mitochondria moved out toward the cell periphery throughout the cell as indicated by the white arrows.

Scale bars, 10 μm.

In this study, we used a CRY2-CIB1 optogenetic system that requires low intensity of blue light and would not induce significant phototoxicity for long-term studies. As we have shown previously, CRY2-CIB1 can dimerize at light intensity as low as 25 $\mu W/cm^2$, and 36-hr continuous illumination of light at 200 $\mu W/cm^2$ induced minimal phototoxicity to PC12 cells (Zhang et al., 2014). We have carried out preliminary tests of the suitability of our method for long-term investigation of organelle redistribution. When COS-7 cells transfected with either CRY2-mCherry-MiroTM/BICDN-GFP-CIB1 or CRY2-mCherry-MiroTM/KIF5A-GFP-CIB1 were placed under 150 $\mu W/cm^2$ blue light for 24 hr, the death rates for cells with sustained molecular motor recruitments were similar to those for dark controls (Figure S6). The suitability for long-term experiments would be particularly useful in studying the role of organelle redistributions in cell events that proceed over a relatively long span of time, such as development of cell polarity and elongation of axons, which usually take days to complete.

It is worth noting that CRY2 undergoes homo-oligomerization in addition to CRY2-CIB1 heterodimerization on exposure to

(D) The average moving distances of mitochondria after 15 min of intermittent blue-light illumination were calculated and plotted along with motor expression level. In 20 cells double-transfected with CRY2-mCherry-MiroTM and KIF5A-GFP-CIB1, the higher was the KIF5A expression level, the further the mitochondria moved toward the cell periphery at the end of the 15-min period (left graph). However, in 17 cells transfected with CRY2P-mCherry-MiroTM and GFP-BICDN-CIB1, the expression level of BICDN had no obvious influence on how far mitochondria moved toward the cell nucleus during the 15-min period (right graph). Scale bars, 10 μm. See also Movie S5.

blue light (Bugaj et al., 2013; Kim et al., 2014; Lee et al., 2014), which could potentially complicate the results obtained from CRY2-CIB1 interaction. However, in this work the CRY2 homo-oligomerization did not interfere with our results. Regardless of whether organelle-localized CRY2 undergoes homo-oligomerization or not, it does not prevent the binding between CRY2 and CIB1. Therefore, our strategy based on CRY2-CIB1 binding to drive organelles in cells is robust and reproducible.

In this study, to control cargo movements, CIB1 was fused to either truncated kinesin or a dynein adaptor protein, BICDN. The truncated kinesin is known to be constitutively active, which means it may occupy microtubule binding sites excessively and thus possibly prevent endogenous molecular motors from attaching to microtubules (Cai et al., 2007). By comparison, overexpression of BICDN will not induce competition between transfected proteins and endogenous molecular motors. However, in our experiments we did not observe any obvious toxicity induced from the overexpression of either plasmid after 2 days.

The findings presented here agree very well with a recent report that controlling organelle redistribution in cells is feasible through optogenetics (van Bergeijk et al., 2015). The optogenetic systems used in the two studies are different: van Bergeijk et al. used the dimerization of LOV2 and engineered PDZ while our method is based on the binding of CRY2/CIB1. In a benchmark study that directly compared the LOV and the CRY2/CIB1 systems, the CRY2 system showed lower background activation and less toxicity than some systems (Pathak et al., 2014). Our study also shows that CRY2/CIB1 system is suitable for long-term experiments.

In conclusion, we provide an optogenetic strategy for controlling motor activities and organelle distribution in living cells with reversibility, spatiotemporal control, and minimal toxicity. This method will be useful in studying organelle transport and the biological importance of organelle distribution.

SIGNIFICANCE

Increasing evidence indicates that organelle transport and distribution plays important roles in various cellular activities. However, establishing a direct link between organelle distribution and cellular functions is hindered by the lack of means to manipulate molecular motors in the complex intracellular environment. Here, we provide an optogenetic strategy to control the transport and distribution of organelles by light, in which blue light induces recruitment of molecular motors onto organelles based on the heterodimerization of *A. thaliana* CRY2 and CIB1. This optical approach has outstanding advantages, such as minimal side effects, reversibility, and precise spatiotemporal control. In this article, we demonstrated that various organelles, including mitochondria, peroxisomes, and lysosomes, can be driven toward the cell periphery or the cell nucleus upon recruitment of specific molecular motors. We confirmed that light-recruited molecular motors move along microtubules, and showed that the light-inducible motor recruitment and organelle movements are repeatable and reversible. We also demonstrated that organelle redistribution can be spatially controlled at subcellular regions. In summary, the optogenetic strategy in this report offers precise and reversible light control of molecular motors and organelle transport in vivo, thus providing a valuable tool to unveil the role of distributions of various organelles in many cellular functions.

EXPERIMENTAL PROCEDURES

Plasmid Construction

All the plasmids used in this study were cloned in the mammalian expression vector pEGFPN1 or pmCherryC1. In this study, light-induced dimerization was based on a truncated CRY2 consisting of the photolyase homology region alone and an N-terminal region of CIB1. Details of all DNA plasmids used in this work are summarized in Table S1A.

GFP-CIB1, CIB1-GFP, and mCherry-CRY2 were firstly made by ligation and used as templates for construction of other plasmids that contain these genes. CRY2-mCherry-Miro1TM was made by inserting the transmembrane domain of Miro1 into CRY2-mCherry using InFusion cloning kit (Clontech). LAMP-mCherry-CRY2 and PEX-mCherry-CRY2 were constructed by inserting LAMP or PEX into mCherry-CRY2 using ligation and InFusion, respectively. KIF5A segment was inserted into GFP-CIB1 to make KIF5A-GFP-CIB1 by ligation. GFP-BICDN-CIB1 was made by inserting BICDN into GFP-CIB1 by InFusion. CIB1-GFP-MiroTM was constructed by inserting MiroTM into CIB1-GFP-Caax by two-step overlapping extension PCR (Bryksin and Matsumura, 2010). The details for plasmid construction are summarized in Table S1B.

Cell Culture and Transfection

COS-7 cells were cultured in DMEM supplemented with 10% fetal bovine serum. All the cell cultures were maintained in a standard humidified incubator at 37°C with 5% CO_2. 1–2 days before transfection, CO7 cells were plated on PLL-coated coverslip and allowed to reach 80% confluence. Cells were transfected with desired DNA plasmids using Lipofectamine 2000 (Life Technologies) according to the manufacturer's protocol. The transfected cells were allowed to recover and express the desired proteins. Fluorescence imaging of the transfected cells was carried out 1 day after transfection.

Live Cell Imaging

Live cell imaging was performed on an epifluorescence microscope (Leica DMI6000B) equipped with an on-stage CO_2 incubation chamber (Tokai Hit GM-8000) and a motorized stage (Prior). Cells plated on coverslips were maintained in standard medium at 37°C with 5% CO_2 during imaging. An adaptive focus control was used to actively keep the image in focus for long-term imaging. A light-emitting diode (LED) light source (Lumencor Sola) was used for fluorescence light source. For blue-light stimulation, pulsed blue light (200-ms pulse duration per 10-s interval at 9.7 W/cm^2) was used for initiating CRY2-CIB1 binding and GFP imaging unless noted otherwise. For mCherry imaging, pulsed green light (200-ms pulse duration) was used at intervals of 10 s or 1 s depending on frame rate of the movie acquisition. The green light used for imaging mCherry does not stimulate CRY2-CIB1 binding, confirming previous findings (Kennedy et al., 2010). Fluorescence signal from GFP was detected using the commercial GFP filter cube (Leica; excitation filter 472/30, dichroic mirror 495, emission filter 520/35); fluorescence signal from mCherry was detected using the commercial Texas red filter cube (Leica; excitation filter 560/40, dichroic mirror 595, emission filter 645/75). All the images were acquired with an oil-immersion 100× objective (Leica; HCX PL APL, n.a. 1.4) and imaged with a sensitive CMOS camera (PCO.EDGE 5.5) (PCO).

Quantitative Determination of Mitochondria Distribution from Cell Nucleus

Mitochondria were labeled by CRY2-mCherry-MiroTM. Using ImageJ, double-transfected cells were extracted from the original images and pasted to a black background to eliminate signal interference from neighboring cells. As shown in Figure S3, a ring that just covered the nucleus was picked and defined as the nucleus in measurement. Using a custom-written MATLAB program, CRY2-mCherry-MiroTM fluorescence signal was segmented into nucleocentric rings of equal width from the nucleus toward the periphery of the cells (Figure S3). The total intensity within each ring indicated the abundance of mitochondria

located in that ring. The percentage of mitochondria within a certain ring, P_l, was calculated as the ratio of the total intensity within that ring versus the total intensity of the whole cell, where the total intensity of the whole cell did not include the intensity inside the nuclear ring. The average distance of all the mitochondria in the cell with respect to the nucleus was calculated as the weighted distance $L_{avg} = \sum_{l=0}^{l} l \times P_l$. l was calculated as the difference between the radius of the nucleocentric ring and that of the nuclear ring.

Determination of KIF5A-GFP-CIB1 and GFP-BICDN-CIB1 Expression Level

Expression levels for GFP-BICDN-CIB1 and KIF5A-GFP-CIB1 were proportional to the GFP fluorescence intensity. Imaging conditions were kept consistent for GFP signal capture. After manually defining the whole cell area and selecting a background area, the ImageJ "Measurement" function was used to measure the average intensity of the GFP fluorescence signal in a transfected cell I_{cell} and that of the background $I_{background}$. The expression level was calculated as the ratio of GFP intensity inside the cell over the background intensity of the image ($I_{cell}/I_{background}$).

Analysis of CRY2-CIB1 Binding Kinetics

For kinetic analysis of CRY2-CIB1 dimerization on organelle membrane, an individual mitochondrion was manually selected. The average mCherry fluorescence intensity of the selected mitochondrion was measured. The mCherry signal increases as the blue light recruits mCherry-CRY2 to the surface of mitochondria until the recruitment saturates at I_{max}. Then the blue-light illumination is stopped and the mCherry intensity decreases as the CRY2-CIB1 dissociate in the absence of blue light until the dissociation is complete at I_{min}. The time-dependent binding percentage of CRY2-CIB1 was calculated as the ratio of the difference between mCherry intensity at time t $I_{(t)}$ and the minimum intensity to the difference between maximum mCherry intensity and minimum intensity:

$$R_{(t)} = \frac{I_{(t)} - I_{\min}}{I_{\max} - I_{\min}}.$$

Cell Cultures and LED Array Setup for Long-Term Light Stimulation

COS-7 cells were plated in six-well plate 1 day before transfection. 6 hr after transfection, cells in each well were split into three 12-well plates, one well per plate. In this way, we obtained three sets of COS-7 cells with the same cell passage number and under identical transfection conditions. Before the next step, the cells were allowed to recover in the dark for 12 hr.

For the long-term blue-light illumination setup, a 2 × 2 blue LED array was built by assembling four blue LEDs (B4304H96, Linrose Electronics) on a breadboard. The LED device was controlled by a LabVIEW program with a data acquisition board (National Instrument-DAQ, PCI-6035E). The LEDs were supplied with user-defined DC voltages that were controlled through the LabVIEW program. The breadboard was kept in an aluminum box. A light-diffuser film was placed on top of the LED array to make the light intensity homogeneous. The average light intensity illuminated to cell cultures was measured by a power meter (Newark, 1931-C). The light intensity in the LED array was set at 150 $\mu W/cm^2$.

Data Acquisition and Analysis of Cell Death Rate

Using the COS-7 cell culturing method mentioned above, two 12-well pates were prepared, each of which contained a set of two co-transfection groups. The two pairs of plasmids for transfection were CRY2-mCherry-MiroTM & BICDN-GFP-CIB1, and CRY2-mCherry-MiroTM & KIF5A-GFP-CIB1. For cell death measurement, one plate was placed on the blue LED array for 24-hr continuous blue-light illumination before imaging. The other plate was incubated in dark for 24 hr and imaged as the 24-hr dark control.

For cell death measurement, cells were incubated in DMEM containing 1 μg/ml propidium iodide (PI) for 20 min. After washing with PBS twice, cells were changed to DMEM for imaging. Using the Leica on-stage automatic setup, an area close to the center of the well was imaged and 36 frames of images were acquired for both GFP and mCherry channels. For the mCherry images, the CRY2-mCherry-MiroTM signal was so weak compared with the PI signal that it could be filtered off by adjusting the image contrast. For almost all transfected cells, cells were co-transfected rather than single-transfected. Thus, the GFP signal from BICDN-GFP-CIB1 or KIF5A-GFP-CIB1 was used to find co-transfected cells. GFP images and mCherry images were merged using ImageJ. Cells with PI stains inside the nucleus were considered as dead cells; otherwise they were considered as living cells. Dead cells and living cells were counted using the "CellCounter" function in ImageJ. Only transfected cells were counted. Cell death ratio was calculated as the number of dead transfected cells over the total number of transfected cells.

SUPPLEMENTAL INFORMATION

Supplemental Information includes six figures, one table, and five movies and can be found with this article online at http://dx.doi.org/10.1016/j.chembiol.2015.04.014.

AUTHOR CONTRIBUTIONS

L.D., D.C., and B.C. conceived and designed the experiments. L.D. made the plasmids. L.D., D.C., K.Z., Q.O., and S.G. performed the experiments. L.D. analyzed the data. D.C. wrote the MATLAB program. L.D., D.C., and B.C. wrote the paper.

ACKNOWLEDGMENTS

We thank Dr. Chandra Tucker (University of Colorado, Denver) for providing CIB1-GFP-Caax and CRY2-mCherry, Dr. Xinnan Wang (Stanford University) for providing Miro1 plasmid, and Dr. Casper Hoogenraad (Utrecht University) for providing plasmids encoding KIF5A, BICDN, and PEX. We also thank Zhuoluo Feng (Stanford University) for his help in constructing the controllable blue LED array. This work was supported by the US NIH (DP2-NS082125) and a Packard fellowship in Science and Engineering.

Received: March 17, 2015
Revised: April 17, 2015
Accepted: April 17, 2015
Published: May 8, 2015

REFERENCES

Al-Mehdi, A.B., Pastukh, V.M., Swiger, B.M., Reed, D.J., Patel, M.R., Bardwell, G.C., Pastukh, V.V., Alexeyev, M.F., and Gillespie, M.N. (2012). Perinuclear mitochondrial clustering creates an oxidant-rich nuclear domain required for hypoxia-induced transcription. Sci. Signal. *5*, ra47.

Boldogh, I.R., and Pon, L.A. (2006). Interactions of mitochondria with the actin cytoskeleton. Biochim. Biophys. Acta *1763*, 450–462.

Bradke, F., and Dotti, C.G. (1997). Neuronal polarity: vectorial cytoplasmic flow precedes axon formation. Neuron *19*, 1175–1186.

Bryksin, A.V., and Matsumura, I. (2010). Overlap extension PCR cloning: a simple and reliable way to create recombinant plasmids. Biotechniques *48*, 463–465.

Bugaj, L.J., Choksi, A.T., Mesuda, C.K., Kane, R.S., and Schaffer, D.V. (2013). Optogenetic protein clustering and signaling activation in mammalian cells. Nat. Methods *10*, 249–252.

Cai, D.W., Hoppe, A.D., Swanson, J.A., and Verhey, K.J. (2007). Kinesin-1 structural organization and conformational changes revealed by FRET stoichiometry in live cells. J. Cell Biol. *176*, 51–63.

Chen, J.W., Cha, Y., Yuksel, K.U., Gracy, R.W., and August, J.T. (1988). Isolation and sequencing of a cDNA clone encoding lysosomal membrane glycoprotein mouse LAMP-1. Sequence similarity to proteins bearing oncodifferentiation antigens. J. Biol. Chem. *263*, 8754–8758.

Fransson, A., Ruusala, A., and Aspenstom, P. (2006). The atypical Rho GTPases Miro-1 and Miro-2 have essential roles in mitochondrial trafficking. Biochem. Biophys. Res. Commun. *344*, 500–510.

Harper, S.M., Neil, L.C., and Gardner, K.H. (2003). Structural basis of a phototropin light switch. Science *301*, 1541–1544.

Idevall-Hagren, O., Dickson, E.J., Hille, B., Toomre, D.K., and De Camilli, P. (2012). Optogenetic control of phosphoinositide metabolism. Proc. Natl. Acad. Sci. USA *109*, E2316–E2323.

Kakumoto, T., and Nakata, T. (2013). Optogenetic control of PIP3: PIP3 is sufficient to induce the actin-based active part of growth cones and is regulated via endocytosis. PLoS One *8*, e70861.

Kammerer, S., Holzinger, A., Welsch, U., and Roscher, A.A. (1998). Cloning and characterization of the gene encoding the human peroxisomal assembly protein Pex3p. FEBS Lett. *429*, 53–60.

Kapitein, L.C., Schlager, M.A., Kuijpers, M., Wulf, P.S., van Spronsen, M., MacKintosh, F.C., and Hoogenraad, C.C. (2010a). Mixed microtubules steer dynein-driven cargo transport into dendrites. Curr. Biol. *20*, 290–299.

Kapitein, L.C., Schlager, M.A., van der Zwan, W.A., Wulf, P.S., Keijzer, N., and Hoogenraad, C.C. (2010b). Probing intracellular motor protein activity using an inducible cargo trafficking assay. Biophys. J. *99*, 2143–2152.

Kennedy, M.J., Hughes, R.M., Peteya, L.A., Schwartz, J.W., Ehlers, M.D., and Tucker, C.L. (2010). Rapid blue-light-mediated induction of protein interactions in living cells. Nat. Methods *7*, 973–975.

Kim, N., Kim, J.M., Lee, M., Kim, C.Y., Chang, K.Y., and Heo, W.D. (2014). Spatiotemporal control of fibroblast growth factor receptor signals by blue light. Chem. Biol. *21*, 903–912.

Konermann, S., Brigham, M.D., Trevino, A.E., Hsu, P.D., Heidenreich, M., Cong, L., Platt, R.J., Scott, D.A., Church, G.M., and Zhang, F. (2013). Optical control of mammalian endogenous transcription and epigenetic states. Nature *500*, 472–476.

Korolchuk, V.I., Saiki, S., Lichtenberg, M., Siddiqi, F.H., Roberts, E.A., Imarisio, S., Jahreiss, L., Sarkar, S., Futter, M., Menzies, F.M., et al. (2011). Lysosomal positioning coordinates cellular nutrient responses. Nat. Cell Biol. *13*, 453–460.

Kural, C., Kim, H., Syed, S., Goshima, G., Gelfand, V.I., and Selvin, P.R. (2005). Kinesin and dynein move a peroxisome in vivo: a tug-of-war or coordinated movement? Science *308*, 1469–1472.

Lee, S., Park, H., Kyung, T., Kim, N.Y., Kim, S., Kim, J., and Heo, W.D. (2014). Reversible protein inactivation by optogenetic trapping in cells. Nat. Methods *11*, 633–636.

Levskaya, A., Weiner, O.D., Lim, W.A., and Voigt, C.A. (2009). Spatiotemporal control of cell signalling using a light-switchable protein interaction. Nature *461*, 997–1001.

Mellman, I., and Nelson, W.J. (2008). Coordinated protein sorting, targeting and distribution in polarized cells. Nat. Rev. Mol. Cell Biol. *9*, 833–845.

Pathak, G.P., Strickland, D., Vrana, J.D., and Tucker, C.L. (2014). Benchmarking of optical dimerizer systems. ACS Synth. Biol. *3*, 832–838.

Quintana, A., Schwarz, E.C., Schwindling, C., Lipp, P., Kaestner, L., and Hoth, M. (2006). Sustained activity of calcium release-activated calcium channels requires translocation of mitochondria to the plasma membrane. J. Biol. Chem. *281*, 40302–40309.

Renicke, C., Schuster, D., Usherenko, S., Essen, L.O., and Taxis, C. (2013). A LOV2 domain-based optogenetic tool to control protein degradation and cellular function. Chem. Biol. *20*, 619–626.

Rizzuto, R., Nakase, H., Darras, B., Francke, U., Fabrizi, G.M., Mengel, T., Walsh, F., Kadenbach, B., Dimauro, S., and Schon, E.A. (1989). A gene specifying subunit-VIII of human cytochrome-c oxidase is localized to chromosome-11 and is expressed in both muscle and non-muscle tissues. J. Biol. Chem. *264*, 10595–10600.

Samsonov, A., Yu, J.Z., Rasenick, M., and Popov, S.V. (2004). Tau interaction with microtubules in vivo. J. Cell Sci. *117*, 6129–6141.

Schwindling, C., Quintana, A., Krause, E., and Hoth, M. (2010). Mitochondria positioning controls local calcium influx in T cells. J. Immunol. *184*, 184–190.

Shimizu-Sato, S., Huq, E., Tepperman, J.M., and Quail, P.H. (2002). A light-switchable gene promoter system. Nat. Biotechnol. *20*, 1041–1044.

Strickland, D., Yao, X.L., Gawlak, G., Rosen, M.K., Gardner, K.H., and Sosnick, T.R. (2010). Rationally improving LOV domain-based photoswitches. Nat. Methods *7*, 623–626.

Strickland, D., Lin, Y., Wagner, E., Hope, C.M., Zayner, J., Antoniou, C., Sosnick, T.R., Weiss, E.L., and Glotzer, M. (2012). TULIPs: tunable, light-controlled interacting protein tags for cell biology. Nat. Methods *9*, 379–384.

Toettcher, J.E., Weiner, O.D., and Lim, W.A. (2013). Using optogenetics to interrogate the dynamic control of signal transmission by the Ras/Erk module. Cell *155*, 1422–1434.

van Bergeijk, P., Adrian, M., Hoogenraad, C.C., and Kapitein, L.C. (2015). Optogenetic control of organelle transport and positioning. Nature *518*, 111–114.

van Spronsen, M., Mikhaylova, M., Lipka, J., Schlager, M.A., van den Heuve, D.J., Kuijpers, M., Wulf, P.S., Keijzer, N., Demmers, J., Kapitein, L.C., et al. (2013). TRAK/Milton motor-adaptor proteins steer mitochondrial trafficking to axons and dendrites. Neuron *77*, 485–502.

Wu, Y.I., Frey, D., Lungu, O.I., Jaehrig, A., Schlichting, I., Kuhlman, B., and Hahn, K.M. (2009). A genetically encoded photoactivatable Rac controls the motility of living cells. Nature *461*, 104–108.

Zhang, K., Duan, L., Ong, Q., Lin, Z., Varman, P.M., Sung, K., and Cui, B. (2014). Light-mediated kinetic control reveals the temporal effect of the Raf/MEK/ERK pathway in PC12 cell neurite outgrowth. PLoS One *9*, e92917.

